Appl. Phys. B 89, 195–200 (2007)
DOI: 10.1007/s00340-007-2784-6

Applied Physics B
Lasers and Optics

U. TANAKA[1,2,✉]
I. MORITA[1]
S. URABE[1,2]

Selective loading and laser cooling of rare calcium isotope $^{43}Ca^{+}$

[1] Graduate School of Engineering Science, Osaka University, 1-3 Machikaneyama, Toyonaka, Osaka 560-8531, Japan
[2] JST-CREST, 4-1-8, Hon-cho Kawaguchi, Saitama 332-0012, Japan

Received: 7 July 2007/Revised version: 24 August 2007
Published online: 3 October 2007 •

ABSTRACT We report a method for loading $^{43}Ca^{+}$ ions selectively in a linear Paul trap using ultraviolet light-emitting-diodes (LEDs) for the second excitation in a two-step photo-ionization process. The difficulty in working with $^{43}Ca^{+}$ is its low natural abundance (0.135%). In order to load $^{43}Ca^{+}$ selectively, we utilize the isotope shifts for the $4s^2\,{}^1S_0$–$4s4p\,{}^1P_1$ transition of neutral calcium atoms. We discuss the limitation of the selectivity of the employed photo-ionization scheme and observe spectra from unwanted isotopes as well as that from $^{43}Ca^{+}$. Purification of $^{43}Ca^{+}$ is performed by adjusting the detuning of the cooling laser frequency and trapping potential. The method of loading and purification can be used in the application of trapped $^{43}Ca^{+}$ for an optical frequency standard and for quantum information processing.

PACS 32.80.Fb; 32.80.Pj

1 Introduction

A string of laser-cooled ions in a linear Paul trap have been considered as a promising system for the development of quantum information processing (QIP) [1, 2]. Calcium ion has been considered as one of the attractive candidates for an optical frequency standard and QIP [3, 4].

Among the naturally occurring calcium isotopes (Table 1), fundamental experiments for the development of frequency standards and demonstrations of QIP using calcium ions have been achieved with the $^{40}Ca^{+}$ isotope [5] because of its high natural abundance of 96.9%. However, the odd isotope $^{43}Ca^{+}$ with a nuclear spin of $I = 7/2$ is a candidate for an optical frequency standard as well as for QIP due to its hyperfine structure. We can select the $M_F = 0$–$M'_F = 0$ transition which is not affected by the first-order Zeeman effect. Moreover, this ion also has a number of advantages as a qubit. In the case of using $^{40}Ca^{+}$ as a qubit, the $S_{1/2}$ ground state and the $D_{5/2}$ metastable state with a natural lifetime of about 1 s are often selected for the two internal levels. While in the case of using $^{43}Ca^{+}$, the $S_{1/2}$ ($F = 3$ and 4) ground states are selected. The lifetime of these two ground states is much longer than the $D_{5/2}$ state of $^{40}Ca^{+}$. For qubit manipulation of $^{40}Ca^{+}$, the 729 nm laser frequency used for the quadrupole transition between the $S_{1/2}$ ground state and the metastable $D_{5/2}$ state has to be highly stabilized, while the manipulation of $^{43}Ca^{+}$ is achieved by driving Raman transitions between the $S_{1/2}$ ($F = 3$ and 4) ground states. If the Raman transitions are driven with a single light source utilizing frequency modulation, the manipulation is less affected by the effect of laser frequency fluctuations. However, the obvious difficulty in working with $^{43}Ca^{+}$ is its low natural abundance of 0.135%. It is also demanding that more lasers have to be prepared to perform the laser cooling of $^{43}Ca^{+}$ than the laser cooling of even isotopes because of the hyperfine structure.

Photo-ionization for loading the calcium ions into a Paul trap was performed by several groups [6–10]. Besides the isotope selectivity, photo-ionization has a number of advantages over electron bombardment ionization. Since no electron beam is involved, there is no charging of insulating parts of the trap structure and reduction of unwanted material sputtered onto the trap electrodes from the oven due to its high efficiency. Clean electrode surfaces are important to reduce the heating rate of trapped ions from the motional ground state [9–11]. Gulde et al. demonstrated a selective photo-ionization scheme with the $4s^2\,{}^1S_0$–$4s4p\,{}^1P_1$ transition at 423 nm followed by the excitation into the continuum by the ultraviolet radiation near 390 nm, and showed that photo-ionization is more efficient than the electron bombardment ionization [9]. Lucas et al. demonstrated that the photo-ionization scheme is capable of loading $^{43}Ca^{+}$ [10].

So far, it has been reported that an incoherent light source is available for the second excitation of the photo-ionization of ^{40}Ca [10] and rare even isotopes [12]. In this paper, we report selective loading of the rare odd isotope $^{43}Ca^{+}$ using a high-power light emitting diode (LED) for the second excitation in the photo-ionization process. We discuss the limitation of selectivity of the employed photo-ionization scheme in which the $4s^2\,{}^1S_0$–$4s4p\,{}^1P_1$ transition at 423 nm is used for the first excitation. To overcome the limitation, we demonstrate purification of $^{43}Ca^{+}$ by adjusting the detuning of cooling laser frequency and trapping potential.

✉ Fax: +81-6-6850-6341, E-mail: utako@ee.es.osaka-u.ac.jp

Mass number	Natural abundance (%)	Isotope shifts (MHz) Ca $4s^2\,{}^1S_0$–$4s4p\,{}^1P_1$	^{43}Ca shift from the center of gravity (MHz)
40	96.9	0	
42	0.647	394	
43	0.135	612	
		(center of gravity)	$(F = 7/2$–$F' = 9/2) - 55$
			$(F = 7/2$–$F' = 7/2) + 18$
			$(F = 7/2$–$F' = 5/2) + 68$
44	2.09	774	
46	0.004	1160	
48	0.187	1513	

TABLE 1 Abundances of the naturally occurring calcium isotopes and isotope shifts for the $4s^2\,{}^1S_0$–$4s4p\,{}^1P_1$ transition at 423 nm

2 Photo-ionization and laser cooling

The schematic diagrams of energy levels of neutral calcium and of singly ionized calcium are shown in Fig. 1a and b, respectively. Isotope selectivity is achieved by use of the isotope shifts for the $4s^2\,{}^1S_0$–$4s4p\,{}^1P_1$ transition (Table 1). A 423 nm violet diode laser is available for excitation of the transition. The second step of the photo-ionization is achieved by a photon near 390 nm [9]. Not only a coherent laser source but also an incoherent light source is available for the second excitation [10, 12]. In our setup, the second excitation is driven with high power LEDs.

Since the natural linewidth of the $4s^2\,{}^1S_0$–$4s4p\,{}^1P_1$ transition (35 MHz) is sufficiently small compared with the isotope shifts, it is expected that high selectivity of isotopes is achieved. In practice, however, purification is necessary due to a high natural abundance of $^{40}Ca^+$ compared with other isotopes and the broadening of the transition.

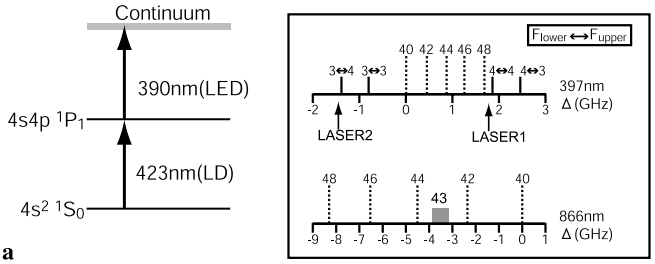

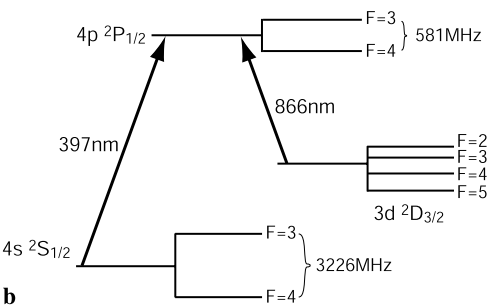

FIGURE 1 Schematic diagram of energy levels of (**a**) neutral even calcium isotopes and (**b**) singly ionized even calcium isotopes and odd calcium isotope. Relevant wavelengths for photo-ionization are also shown. *Inset*: Frequency locations of the hyperfine components of the 397 nm transition and the isotope shifts of the even isotopes as a function of detuning Δ relative to $^{40}Ca^+$. The hyperfine components are indicated by *solid lines*. The isotope shifts of the even isotopes are indicated by *dotted lines* and labeled with the mass number. The detuning of the two 397 nm lasers for the cooling of $^{43}Ca^+$ is shown. The isotope shifts in the 866 nm transition are also shown, without the hyperfine details for $^{43}Ca^+$

We estimated the ratio between the fractional population of the $4s4p\,{}^1P_1$ upper state of even isotope and that of ^{43}Ca as a function of Doppler width and the 423 nm laser intensity. We assumed that the atom was illuminated with a linearly polarized light and that the laser was tuned at the peak of the $^1S_0$ $(F = 7/2)$ to $^1P_1$ $(F' = 9/2)$ hyperfine component of ^{43}Ca. The effect of saturation broadening is given by solving the two-level rate equations of the $^1S_0$ $(J = 0)$–$^1P_1$ $(J' = 1)$ transition for the even isotopes and the four-level rate equations of the $^1S_0$ $(F = 7/2)$–$^1P_1$ $(F' = 9/2, 7/2, 5/2)$ transitions for the odd isotope. The population of the upper level for the even isotopes is

$$\varrho_{ee}^{\text{even}}(\Delta_{423}) = \frac{\frac{\beta(\Omega^{\text{even}})^2}{2A}}{\Delta_{423}^2 + \beta^2 + \frac{\beta(\Omega^{\text{even}})^2}{A}}\,, \tag{1}$$

where Δ_{423} is the detuning, A is the Einstein coefficient for the transition $(A = 2.23 \times 10^8\,\text{s}^{-1})$, $\beta = (2\pi\Gamma_\text{L} + A)/2$ with Γ_L is the laser linewidth, and Ω^{even} is the Rabi frequency for the even isotopes. Here we assumed Γ_L to be 1 MHz. The total population of the upper levels for the odd isotopes is

$$\varrho_{ee}^{\text{odd}}(\Delta_{423}) = \frac{\sum_{i=2}^{4} \frac{R_i}{R_i + A}}{1 + \sum_{i=2}^{4} \frac{R_i}{R_i + A}}\,, \tag{2}$$

with

$$R_i = \frac{\frac{\beta\left(\Omega_i^{\text{odd}}\right)^2}{2}}{(\Delta_{423} - \delta_i)^2 + \beta^2}\,, \quad (i = 2, 3, 4)\,, \tag{3}$$

where i labels the transitions between hyperfine levels, that is, $i = 2$, 3, and 4 represent the $(F = 7/2)$–$(F' = 9/2)$, $(F = 7/2)$–$(F' = 7/2)$, and $(F = 7/2)$–$(F' = 5/2)$ transitions, respectively, δ_i is the difference between the resonance frequency of the transition labeled with i and that of the $^1S_0(F = 7/2)$–$^1P_1$ $(F' = 9/2)$ transition, and Ω_i^{odd} is the Rabi frequency for the transition labeled with i. In the case of even isotopes, the squared Rabi frequency is given by

$$(\Omega^{\text{even}})^2 = \left(\frac{E}{\hbar}\right)^2 \frac{2J' + 1}{2J + 1} \frac{3\varepsilon_0 h c^3}{16\pi^3 \nu^3} \frac{A}{3}\,, \tag{4}$$

where E is the amplitude of the electric field, ε_0 is the dielectric constant, c is the speed of light, and ν is the frequency of light. In the case of odd isotope with nonzero nuclear spin I, the hyperfine interaction should be included. The lower and the upper sublevels are denoted by $|\gamma JIFM_\text{F}\rangle$ and

$|\gamma' J' I F' M'_{\rm F}\rangle$, respectively, where γ represents all the other properties of the state besides its orbital angular momentum. In the presence of degeneracy, the squared Rabi frequency is

$$(\Omega_i^{\rm odd})^2 = \left(\frac{eE}{\hbar}\right)^2 \frac{1}{2F+1} \times \sum_{M_{\rm F}} \sum_{M'_{\rm F}} \left|\langle \gamma J I F M_{\rm F}|\hat{x}|\gamma' J' I F' M'_{\rm F}\rangle\right|^2 , \quad (5)$$

where e is electric charge. This can be rewritten in terms of the line strength $S(\gamma JIF; \gamma' J' IF')$ which is related to the line strength $S(\gamma J; \gamma' J')$ [13]. By using the relation between the $S(\gamma J; \gamma' J')$ and the Einstein coefficient A, we obtain

$$\left(\Omega_i^{\rm odd}\right)^2 = \left(\frac{E}{\hbar}\right)^2 (2F'+1) \left\{ \begin{array}{ccc} J & F & I \\ F' & J' & 1 \end{array} \right\}^2 (2J'+1) \times \frac{3\varepsilon_0 h c^3}{16\pi^3 \nu^3} \frac{A}{3} . \quad (6)$$

The array of quantum numbers in the curly braces is $6j$ symbol. Considering Doppler broadening, the fractional population as a function of detuning Δ_{423} is proportional to the Voigt profile $n(\Delta_{423}, \Omega)$

$$n(\Delta_{423}, \Omega) = \frac{C}{\delta\omega_{\rm D}} \int \exp\left(\frac{-\omega'^2}{(\delta\omega_{\rm D}/2\sqrt{\ln 2})^2}\right) \times \varrho_{ee}(\Delta_{423} - \omega')\, {\rm d}\omega' , \quad (7)$$

where C is a constant and $\delta\omega_{\rm D}$ is the full width at half maximum (FWHM) of the Doppler broadening which depends on the mass of the isotope. We defined the ratio between the fractional population of ^{43}Ca and that of other isotope as

$$R = \frac{\eta_{\rm even} n(\Delta_{423}, \Omega^{\rm even})}{\eta_{43} n(0, \Omega_i^{\rm odd})} , \quad (8)$$

where $\eta_{\rm even}$ and η_{43} are the natural abundances of even isotope and ^{43}Ca, respectively.

Figure 2a and b show the estimated ratios during the photo-ionization process for $^{43}Ca^{+}$ as a function of residual Doppler broadening and 423 nm laser intensity, respectively. In Fig. 2a, the laser intensity is fixed at 0.15 mW/mm^2, while the Doppler width (FWHM) is fixed at 45 MHz in Fig. 2b. In this estimation, $^{48}Ca^{+}$ and $^{46}Ca^{+}$ were neglected since the fractional populations of these isotopes are extremely low. Figure 2a and b indicate that loading of some of unwanted isotopes can not be completely avoided in this photo-ionization scheme even though the laser intensity and residual Doppler broadening are ideally reduced. In particular, further reduction of the Doppler width in this region is not effective for the improvement of isotope selectivity.

After the photo-ionization process, laser cooling is performed with the $S_{1/2}$– $P_{1/2}$ transition at 397 nm and the $P_{1/2}$– $D_{3/2}$ transition at 866 nm as a repumping process (Fig. 1b). In the case of laser cooling of even isotopes, isotope shifts for the $S_{1/2}$– $P_{1/2}$ transition and the $P_{1/2}$– $D_{3/2}$ transition can be utilized for cooling specific isotopes while heating other isotopes by adjusting the detuning of the 397-nm and 866-nm laser frequencies. However, the requirements of laser for laser cooling of $^{43}Ca^{+}$ are more demanding than that for the even isotopes

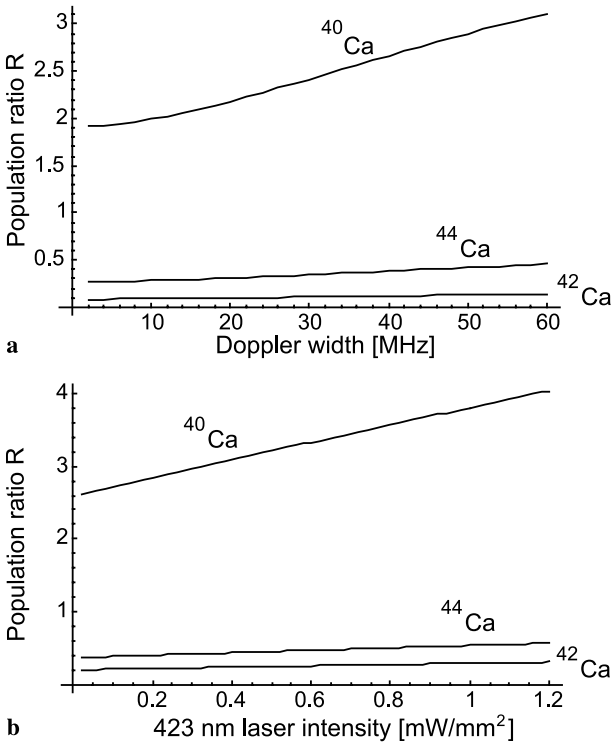

FIGURE 2 Estimated ratio between the fractional population of the $4s4p\,^1P_1$ upper state of the even calcium isotope and that of ^{43}Ca as a function of (**a**) the residual Doppler width (the 423 nm laser intensity is fixed at 0.15 mW/mm^2) and (**b**) the 423 nm laser intensity (the residual Doppler width is fixed at 45 MHz)

because of the hyperfine structure. In particular, a separate repumper is necessary on one of the ultraviolet transitions because of the large (3.2 GHz) hyperfine splitting between the $S_{1/2}$ ($F = 3$ and 4) levels. In our setup, closed cooling cycle of $^{43}Ca^{+}$ is achieved using the $S_{1/2}$ ($F = 4$)– $P_{1/2}$ ($F' = 4$) transition and the $S_{1/2}$ ($F = 3$)– $P_{1/2}$ ($F' = 4$) transition at 397 nm. Because this cooling scheme can be performed only by the transitions at 397 nm and 866 nm, the light sources for other transitions ($S_{1/2}$– $P_{3/2}$, $P_{3/2}$– $D_{3/2}$, and $P_{3/2}$– $D_{5/2}$) are not necessary. Frequency locations of the $^{43}Ca^{+}$ hyperfine components of the 397 nm transitions and the isotope shifts of the even isotopes are shown in the inset of Fig. 1. We select the $S_{1/2}$ ($F = 4$)– $P_{1/2}$ ($F' = 4$) transition as a cooling transition and the $S_{1/2}$ ($F = 3$)– $P_{1/2}$ ($F' = 4$) transition as a repumping transition. The main advantage of using the $S_{1/2}$ ($F = 4$)– $P_{1/2}$ ($F' = 4$) as a cooling transition is that it is blue-detuned from the $S_{1/2}$– $P_{1/2}$ transition in all the even isotopes. It means that any other isotopes that are loaded tend to be heated and that only $^{43}Ca^{+}$ can be cooled. However, the repumping transition $S_{1/2}$ ($F = 3$)– $P_{1/2}$ ($F' = 4$) is red-detuned from the $S_{1/2}$– $P_{1/2}$ transition of any other isotopes. This fact means that any other isotopes are laser-cooled, therefore the repumping 397 nm laser should be irradiated at the lower power than that of the cooling 397 nm laser. Two 397 nm lasers named LASER 1 and LASER 2 are red-detuned from the resonance of cooling transition and the repumping transition, respectively (Fig. 1). Compared with the cooling scheme in [10] in which the $S_{1/2}$ ($F = 4$)– $P_{3/2}$ ($F' = 5$) transition at 393 nm was used for cooling and the $S_{1/2}$ ($F = 3$)– $P_{1/2}$ ($F' = 4$) transition at 397 nm for repumping, the intensity of LASER 2

should be larger (at least by several times) in our scheme. It would affect on the isotope selectivity but we set the intensities of LASER 1 and LASER 2 so that the total effect of the lasers heats the unwanted even isotopes. Repumping from the $D_{3/2}$ levels are achieved with the 866 nm lasers. Since the hyperfine splitting between $D_{3/2}$ ($F = 2$) and $D_{3/2}$ ($F = 5$) is within 600 MHz, repumping can be achieved adequately without preparing the same number of 866 nm lasers as the possible numbers of hyperfine transitions between the $P_{1/2}$ and $D_{3/2}$ levels [10]. In the present setup, we use two 866 nm lasers to repump the ions from the $D_{3/2}$ state efficiently and set their frequencies to be lower than that of the resonance frequency of $^{40}Ca^{+}$ by 3.5 GHz and 3.7 GHz.

3 Experimental apparatus

All of the lasers in our setup, i.e., the light source for the first step of the photo-ionization and those for laser cooling of the ionized calcium, are diode lasers. Each diode laser forms an external-cavity diode laser (ECDL) with a diffraction grating in the Littrow configuration except for one 866 nm repumping laser. One of the 866 nm lasers is a free-running laser. Each ECDL is frequency-stabilized with a temperature-controlled Fabry–Pérot cavity that has a thin Brewster glass plate inside. An error signal obtained by means of the Hänsch–Couillaud method [14] is fed back to the current and the piezoelectric transducer voltage of the ECDL through a PI controller (PID control is applied only for the stabilization of the ECDL for the cooling 397 nm laser). The outputs of the 397 nm ECDLs are reflected with a diffraction grating then passed through a pair of lenses between which a spatial filter with a diameter of 100 μm is set to eliminate background incoherent radiation [15]. The focal length and the numerical aperture of the first lens and the second lens are 200 mm, 0.075, 100 mm, and 0.148, respectively. The spatial mode of the 397 nm cooling laser is filtered by a single-mode fiber.

The second excitation for the photo-ionization is driven with two high power ultraviolet LEDs (Nichia NCCU001E) with the output power of 85 mW, the peak wavelength of 380 nm, and the spectral width of 15 nm. Using a LED is preferable because it is much cheaper than diode laser and no stabilization of current and temperature is required for its operation. However, it is difficult to collimate the output of the LED due to its poor directivity. In order to focus the LED output properly to the ions, a lens system composed of one condenser lens with the focal length of 10 mm and three plano-convex lenses are used. In the current setup, the distance between the LED and the trap center is not the same for the two LEDs. After passing through the vacuum chamber, both beams are reflected back to the trapping region with concave mirrors. Since the image of the LED does not have a Gaussian profile but a complicated structure, it is difficult to accurately measure the intensity at the ion. The estimated averaged intensities at the trapping region of the two LEDs were approximately 20 mW/cm^2 and 5 mW/cm^2, respectively.

The linear trap assembly placed in a vacuum chamber is formed of four cylindrical rods and two dc electrodes at the edge of the rods. The radius and length of the rods are 5 mm and 50 mm, respectively. The perpendicular distance from the trap axis to the trap electrodes is 2.5 mm. The trap is operated with an alternating voltage of 5.4 MHz and 450 V_{amp}. To confine the ions axially, a dc voltage of 50 V is applied to the end electrodes. A calcium oven is set under the trap so that the calcium beam intersects the trapping region perpendicular to the 423 nm laser beam irradiated along the trap axis. Two apertures having 1 mm diameter hole are used for the collimation of the calcium beam to avoid the first-order Doppler shifts in the $4s^2\,{}^1S_0$–$4s4p\,{}^1P_1$ transition. The power of the 423 nm laser beam used was 19 μW. The cooling and repumping 397 nm diode laser beams are overlapped with a polarizing beamsplitter. The 397 nm and 866 nm diode laser beams are overlapped with a dichroic mirror then irradiated to the trapping region from the opposite side to the 423 nm beam. Fluorescence intensity from the neutral atom beam or trapped ions is measured with a photomultiplier and a photon counter. In order to detect only ultraviolet radiation, an interference filter for blocking the near infrared radiation and a spatial filter for reducing the stray scattered light are placed in front of the photomultiplier.

4 Results

A fluorescence spectrum from the neutral calcium beam was obtained by scanning the frequency of the 423 nm laser about 3 GHz. We observed the fluorescence from all of the isotopes other than ^{46}Ca (0.004%). The linewidths (FWHM) of the spectra were approximately 70 MHz. The fact that the linewidth is larger than the natural linewidth is mainly due to the residual Doppler broadening, although we collimate the calcium beam with two apertures.

Selective loading of $^{43}Ca^{+}$ was performed as follows. First we tuned the 423 nm laser frequency to the resonance of the $4s^2\,{}^1S_0 - 4s4p\,{}^1P_1$ transition of ^{43}Ca and maximized the fluorescence from the atomic beam at the oven current of 2.1 A. The LEDs and the laser beams were irradiated to the trapping region for 5 min. After loading, the oven, the 423 nm laser and the LEDs were turned off then the fluorescence was observed with the photomultiplier. The power of the cooling and repumping 397 nm laser beams and two 866 nm laser beams were 140 μW, 60 μW, 3.5 mW and 2.5 mW, respectively. The beam diameters of 397 nm lasers and the 423 nm laser were approximately 70 μm and 140 μm, respectively. The beam diameters of the 866 nm lasers were approximately 110 μm and 280 μm if we assume the beam profile is elliptical Gaussian.

We observed the fluorescence from unwanted isotopes trapped as well as $^{43}Ca^{+}$ for the selective loading of $^{43}Ca^{+}$. After loading $^{43}Ca^{+}$ in the above condition, one of the 866 nm lasers was tuned to the resonance of the $P_{1/2}$– $D_{3/2}$ transition of the other isotopes. The LASER 2 and the other 866 nm laser were detuned same as above. Fluorescence spectra from $^{43}Ca^{+}$ and other isotopes were simultaneously observed by scanning the frequency of LASER 1 by 2.8 GHz to cover the resonance of the all isotopes for the 397 nm transition. Figure 3a and b show the fluorescence spectra obtained by turning the 866 nm laser to the resonance of $^{40}Ca^{+}$ and $^{44}Ca^{+}$, respectively. Two peaks originated from the $S_{1/2}$ ($F = 4$)– $P_{1/2}$ ($F' = 3$) transition and the $S_{1/2}$ ($F = 4$)– $P_{1/2}$ ($F' = 4$) transition of the $^{43}Ca^{+}$ were observed. The reason why $^{40}Ca^{+}$ and

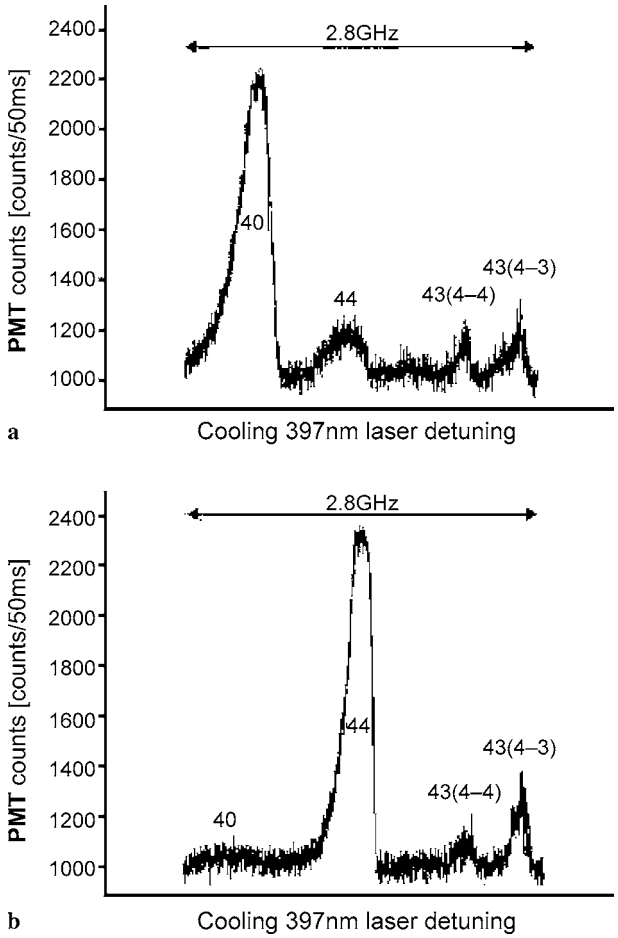

FIGURE 3 Fluorescence spectrum from a mixture of $^{40}Ca^{+}$, $^{43}Ca^{+}$ and $^{44}Ca^{+}$ obtained by scanning the frequency of the cooling 397 nm laser. The repumping 866 nm laser was tuned to (**a**) the resonance of the $P_{1/2}$– $D_{3/2}$ transition of $^{40}Ca^{+}$ and (**b**) the resonance of $P_{1/2}$– $D_{3/2}$ transition of $^{44}Ca^{+}$

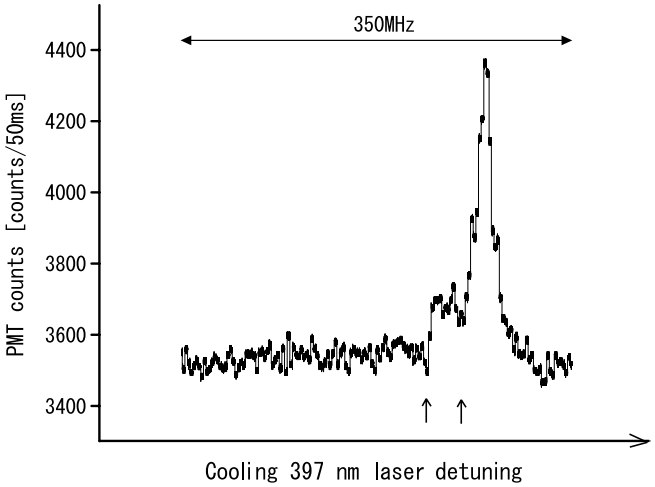

FIGURE 4 Fluorescence spectrum from pure $^{43}Ca^{+}$ crystal obtained by scanning the 397 nm laser frequency. Two dips in the fluorescence (*arrowed*) are probably due to dark resonance

$^{44}Ca^{+}$ were also trapped and laser-cooled is considered to be due to photo-ionization of unwanted isotopes as shown in the estimation in Sect. 2. The ratio between the observed fluorescence intensity from the unwanted isotopes and that from $^{43}Ca^{+}$ is not simply proportional to the estimated ratio shown in Fig. 2. We consider that it is due to the difference in cooling efficiency, the charge exchange, and the sympathetic cooling of other isotopes by $^{43}Ca^{+}$.

To cool $^{43}Ca^{+}$ efficiently, purification of $^{43}Ca^{+}$ from the mixture of $^{43}Ca^{+}$ and unwanted isotopes is necessary. Alheit et al. performed a purification process using nonlinear resonances at certain operating points inside the stability diagram of Paul trap [16]. Hasegawa et al. demonstrated that an additionally applied rf perturbation to excite the secular motion realizes removal of unwanted isotopes [17]. When laser cooling is carried out, laser heating is useful for eliminating unwanted isotopes. Lucas et al. showed an effective purification process in their cooling scheme where the 393 nm laser was chosen for the cooling transition [10]. We carried out purification in a similar manner to the scheme that Toyoda et al. demonstrated for $^{42}Ca^{+}$ and $^{44}Ca^{+}$ in [18]. They separated isotopes by mainly using a selective heating and cooling method in which the isotope shifts were utilized, and then they reduced the trapping potential. We performed laser heating of the unwanted isotopes by tuning the frequency of two 397 nm laser beams and elimination of them by changing the amplitude of the alternating voltage applied to the rod electrodes. First the power of LASER 1 irradiated to the trapped ions was raised up to 490 μW. The frequency of LASER 1 was red-detuned from the $S_{1/2}$ $(F = 4)$– $P_{1/2}$ $(F' = 4)$ transition by approximately 100 MHz. Since LASER 1 was blue-detuned from the resonance of the $S_{1/2}$– $P_{1/2}$ transition of other isotopes, the unwanted isotopes were laser-heated. The power of LASER 2 was 60 μW and the frequency was set to be below the $S_{1/2}$ $(F = 3)$– $P_{1/2}$ $(F' = 4)$ transition by approximately 300 MHz. To heat the isotope we need to eliminate efficiently, one of the 866 nm lasers was tuned to the resonance of the $P_{1/2}$– $D_{3/2}$ transition of the isotope. By decreasing the amplitude of the alternating voltage to 260 V_{amp}, we could eliminate the unwanted isotopes, i.e. $^{40}Ca^{+}$ and $^{44}Ca^{+}$. After purification, the fluorescence from $^{40}Ca^{+}$ and $^{44}Ca^{+}$ was not observed, that is, we could confirm that only $^{43}Ca^{+}$ ions were trapped in the trapping region. This purification process is effective for elimination of unwanted isotopes, however, we note that only a few times we lost not only the unwanted isotopes but also the $^{43}Ca^{+}$.

After purification, laser cooling of $^{43}Ca^{+}$ was performed again as follows. The repumping 397 nm laser was red-detuned from the $S_{1/2}$ $(F = 3)$– $P_{1/2}$ $(F' = 4)$ transition and two 866 nm lasers were set to the frequency range that the excitation from $D_{3/2}$ levels to $P_{1/2}$ levels were driven. Figure 4 shows a fluorescence profile from the pure $^{43}Ca^{+}$ as the frequency of the cooling 397 nm laser was scanned over the $S_{1/2}$ $(F = 4)$– $P_{1/2}$ $(F' = 4)$ transition. The discontinuity of the spectrum represents dark resonance due to the detuning of 397 nm and two 866 nm lasers.

5 Conclusion and outlook

We have performed selective loading of the rare calcium odd isotope $^{43}Ca^{+}$ using a high-power LED as the light sources in the second excitation of the photo-ionization process. We have found that utilizing a LED is available for the photo-ionization of ^{43}Ca in spite of its low natural abun-

dance of 0.135%. We have performed Doppler-cooling of $^{43}Ca^{+}$ that have hyperfine splitting by irradiating the trapped ions with two cooling lasers to achieve a closed cooling cycle. Moreover, we have also observed that the purification of $^{43}Ca^{+}$ is possible by selecting a proper power for the two cooling lasers and alternating the voltage applied to the trap electrodes. Finally, we have observed the fluorescence spectrum from pure $^{43}Ca^{+}$ crystal.

In the future, we will optimize the frequencies and intensities of the lasers to cool $^{43}Ca^{+}$ efficiently. We will also consider a cooling scheme using a microwave transition between two ground states in the hyperfine structure as a repumping process instead of using two 397 nm lasers [19]. The establishment of these techniques is expected to improve the isotope selectivity and the cooling efficiency of $^{43}Ca^{+}$.

REFERENCES

1 J.I. Cirac, P. Zoller, Phys. Rev. Lett. **74**, 4091 (1995)
2 C. Monroe, D.M. Meekhof, B.E. King, W.M. Itano, D.J. Wineland, Phys. Rev. Lett. **75**, 4714 (1995)
3 C. Champenois, M. Houssin, C. Lisowski, M. Knoop, G. Hagel, M. Vedel, F. Vedel, Phys. Lett. A **331**, 298 (2004)
4 M. Kajita, Y. Li, K. Matsubara, K. Hayasaka, M. Hosokawa, Phys. Rev. A **72**, 043 404 (2005)
5 F. Schmidt-Kaler, H. Häffner, M. Riebe, S. Gulde, G.P.T. Lancaster, T. Deuschle, C. Becher, C.F. Roos, J. Eschner, R. Blatt, Nature **422**, 408 (2003)
6 N. Kjærgaard, L. Hornekær, A.M. Thommesen, Z. Videsen, M. Drewsen, Appl. Phys. B **71**, 207 (2000)
7 M. Drewsen, I. Jensen, J. Lindballe, N. Nissen, R. Martinussen, A. Mortensen, P. Staanum, D. Voigt, Int. J. Mass. Spectrom. **229**, 83 (2003)
8 A. Mortensen, J.J.T. Lindballe, I.S. Jensen, P. Staanum, D. Voigt, M. Drewsen, Phys. Rev. A **69**, 042 502 (2004)
9 S. Gulde, D. Rotter, P. Barton, F. Schmidt-Kaler, R. Blatt, W. Hogervorst, Appl. Phys. B **73**, 861 (2001)
10 D.M. Lucas, A. Ramos, J.P. Home, M.J. McDonnell, S. Nakayama, J.-P. Stacey, S.C. Webster, D.N. Stacey, A.M. Steane, Phys. Rev. A **69**, 012 711 (2004)
11 Q.A. Turchette, D. Kielpinski, B.E. King, D. Leibfried, D.M. Meekhof, C.J. Myatt, M.A. Rowe, C.A. Sackett, C.S. Wood, W.M. Itano, C. Monroe, D.J. Wineland, Phys. Rev. A **61**, 063 418 (2000)
12 U. Tanaka, H. Matsunishi, I. Morita, S. Urabe, Appl. Phys. B **81**, 795 (2005)
13 I.I. Sobelman, *Atomic Spectra and Radiative Transitions*, 2nd edn. (Springer, Heidelberg, 1992)
14 T.W. Hänsch, B. Couillaud, Opt. Commun. **35**, 441 (1980)
15 K. Toyoda, A. Miura, S. Urabe, K. Hayasaka, M. Watanabe, Opt. Lett. **26**, 1897 (2001)
16 R. Alheit, K. Enders, G. Werth, Appl. Phys. B **62**, 511 (1996)
17 T. Hasegawa, T. Shimizu, Appl. Phys. B **70**, 867 (2000)
18 K. Toyoda, H. Kataoka, Y. Kai, A. Miura, M. Watanabe, S. Urabe, Appl. Phys. B **72**, 327 (2001)
19 U. Tanaka, S. Urabe, M. Watanabe, Appl. Phys. B **78**, 43 (2004)